

# THE MITIGATION EFFECTS OF LITHIUM AND SODIUM COMPOUNDS ON ALKALI-SILICA REACTION OF CONCRETES

Irfan PRASETIA<sup>\*1</sup>, Kazuyuki TORII<sup>\*2</sup>

## ABSTRACT

The ionic diffusivity of lithium and sodium compounds was investigated by diffusion cell test. The diffusion coefficients of Na<sup>+</sup> ions were 10 times more than Li<sup>+</sup> ions. This is an indication of lithium ions is better adsorbed into the hydration products compared with others, especially Li<sub>2</sub>SiO<sub>3</sub>. This finding is backed-up by results of post-analysis such as DSC and XRD. The results of mortar bar tests were adding confidence to the mitigation effects of lithium on ASR of concrete. Expansions only observed for mortar bars immersed in sodium compounds solution, especially in 0.5 mol/L Na<sub>2</sub>SiO<sub>3</sub>.

**Keywords:** “Through-Diffusion” test, lithium and sodium compounds, diffusion coefficients, ASR mitigation,

## 1. INTRODUCTION

Recently, in New Zealand, lithium and sodium compounds are suggested to be used for reducing the expansion of concrete affected by alkali silica reaction (ASR) [1]. Some research works also confirmed the use of the addition of lithium and sodium compounds for suppressing alkali silica reaction (ASR) in concrete [2,3]. It has also been reported that ASR gel incorporating lithium was less expansive, and that the addition of lithium hydroxide decreased the total amount of ASR gel produced [4,5].

However, in the case of Japan, with the existence of one single supplier of lithium-based compounds in the past (N Chemical Industries, Ltd) which has driven the whole concrete industry into the usage of the highly expensive lithium nitrite (LiNO<sub>2</sub>) for both, ASR mitigation and control of reinforcing steel bar corrosion [6]. Furthermore, in Japan, a bridge pier repaired with Na<sub>2</sub>SiO<sub>3</sub> compound had been discovered re-damaged by ASR as shown in Fig. 1.



Fig.1 Bridge pier repaired with Na<sub>2</sub>SiO<sub>3</sub> compound and subsequently re-damaged by ASR in Toyama Prefecture

There has been a lack of awareness that the hydrolysis reaction of sodium compound and water to produce NaOH is raising the alkalinity in pore solution, which also increases the OH<sup>-</sup> in the solution, thus might triggers the occurrence of ASR. Only a few researchers have been conducted on this matter, thus the mechanism still unclear.

Therefore, this research main objective is to investigate the diffusivity of externally supplied lithium and sodium compounds into cementitious materials and to propose a more economical and effective compound for mitigating ASR. In addition, to find out the effect of lithium and sodium compounds on suppression of ASR expansion, the accelerated mortar bar test according to ASTM C1260 was also carried out for specimens immersed in low and high concentrated lithium and sodium solutions.

## 2. EXPERIMENTS

### 2.1 Materials and Mix Proportions

#### 2.1.1 Diffusion cell test

Cement pastes were prepared with ordinary portland cement (OPC) and the water/cement ratio was set at 40%, which the latter is addressed as OPC-0.4. Two lithium electrolytes sources and two sodium electrolytes sources were selected, which are LiNO<sub>3</sub>, Li<sub>2</sub>SiO<sub>3</sub>, NaNO<sub>3</sub> and Na<sub>2</sub>SiO<sub>3</sub>. The concentrations of LiNO<sub>3</sub> and NaNO<sub>3</sub> solutions were set at 1 mol/L and the concentrations of Li<sub>2</sub>SiO<sub>3</sub> and Na<sub>2</sub>SiO<sub>3</sub> solutions were set at 0.5 mol/L.

#### 2.1.2 Mortar bar test

Crushed calcined flint produced from industrial raw materials in England was used as reactive aggregate, with the grain size ranging from 0.6mm to 2.5mm, and cristobalite as the only reactive component. Regarding

\*1 Graduate School of Natural Science and Technology, Kanazawa University, JCI Student Member

\*2 Prof., Dep. of Env. Design, College of Science & Eng., Kanazawa University, JCI Member

the chemical method in accordance to JIS A1145-2007, the dissolved silica content (Sc) and the reduction in alkaline concentration (Rc) were 1063 mmol/L and 70mmol/L, respectively. Crushed limestone sand with 0.15mm to 5.0mm particle size was used as non-reactive aggregate and considering the pessimum mixing ratio to this calcined flint, the mass ratio of calcined flint to crushed limestone sand was set at 25%:75% [7]. Ordinary Portland cement (T Corporation, Ltd., density: 3.16 g/cm<sup>3</sup>, Blaine specific surface area: 3300 cm<sup>2</sup>/g) was used. The alkali content of the cement was 0.42%.

## 2.2 Test Methods

### 2.2.1 Diffusion cell test

Fig. 2 shows the diffusion cell unit. The cement pastes were cast into PVC acrylic rings, 5mm thick and 30mm internal diameter, placed on glass plates, manually compacted and covered for one day to prevent early dryness and water loss. The cement pastes were then allowed to cure in Ca(OH)<sub>2</sub> saturated water solution for 7, 28 and 91 days, under room temperature of 20 °C and 60% R.H. The diffusion experiments were carried out by Through Diffusion Cell Test. Diffusion cells were setup by adding 100ml of electrolyte sources of lithium and sodium solutions in the tracer cell (cell on the right side) and 100ml of de-ionized water in the measurement cell (cell on the left side) with the cement paste forming the partition between the two sides. After 24 hours, first sampling was performed and the procedure was repeated every 2 days afterwards. The ionic concentration was measured by a PIA-1000 ion analyzer.

### 2.2.2 Mortar bar test

In order to assess the effects of lithium and sodium compounds on suppression of ASR expansion, the accelerated mortar bar tests in accordance to ASTM C1260 method were conducted for specimens immersed in a low (0.5 mol/L) and high (2.5 mol/L) concentrated Li<sub>2</sub>SiO<sub>3</sub> and Na<sub>2</sub>SiO<sub>3</sub> solutions and also for specimens immersed in a low (1 mol/L) concentrated NaNO<sub>3</sub>.

## 3. RESULTS AND DISCUSSION

### 3.1 Diffusion Cell Test

#### 3.1.1 Diffusion Profiles

Fig. 3 shows the diffusion profiles of Li<sup>+</sup> ions from LiNO<sub>3</sub> and Li<sub>2</sub>SiO<sub>3</sub> solution into 7, 28 and 91 days aged OPC-0.4 samples. Whereas Fig. 4 shows the diffusion profiles of Na<sup>+</sup> ions from NaNO<sub>3</sub> and Na<sub>2</sub>SiO<sub>3</sub> solutions into 7, 28 and 91 days aged OPC-0.4 samples. In the case of lithium solutions, the diffusion gradients were rise steeply for LiNO<sub>3</sub> solution at 28 days curing time and Li<sub>2</sub>SiO<sub>3</sub> solution at 7 days curing time. As for LiNO<sub>3</sub> solution at 7 and 91 days curing time and Li<sub>2</sub>SiO<sub>3</sub> solution at 28 and 91 curing time are less evident. The diffusion gradients decreased considerably with curing time, as opposed to NaNO<sub>3</sub> and Na<sub>2</sub>SiO<sub>3</sub> solution. This can be seen clearly at diffusion of Na<sup>+</sup> ion of NaNO<sub>3</sub> solution. The diffusion concentration is large at 28 days curing time, but become little at 91 days curing time. It shows that over time NaNO<sub>3</sub> solution is absorbed well

into the hydration products. The amount even similar to the diffusion profiles of Li<sup>+</sup> ions from LiNO<sub>3</sub> and Li<sub>2</sub>SiO<sub>3</sub> solution. Overall, the concentration of sodium solutions was 10x more than lithium solutions.

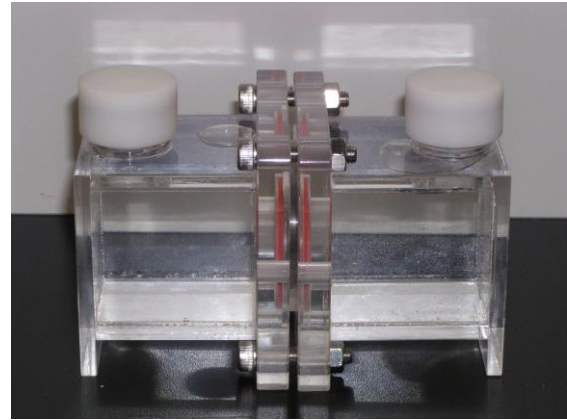


Fig. 2 Diffusion cell unit used in this study

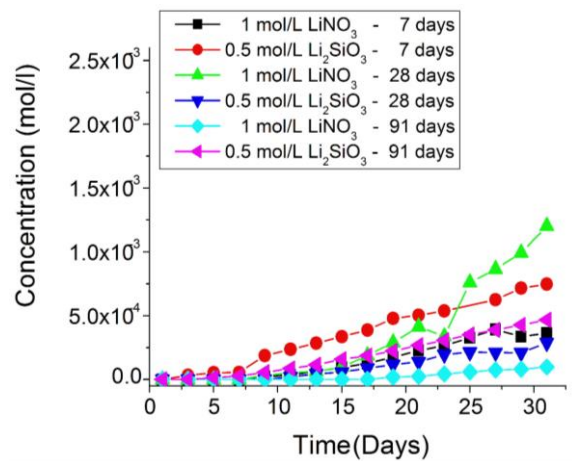


Fig. 3 Diffusion profiles of Li<sup>+</sup> ions from LiNO<sub>3</sub> and Li<sub>2</sub>SiO<sub>3</sub> solution (curing time: 7, 28 and 91 days)

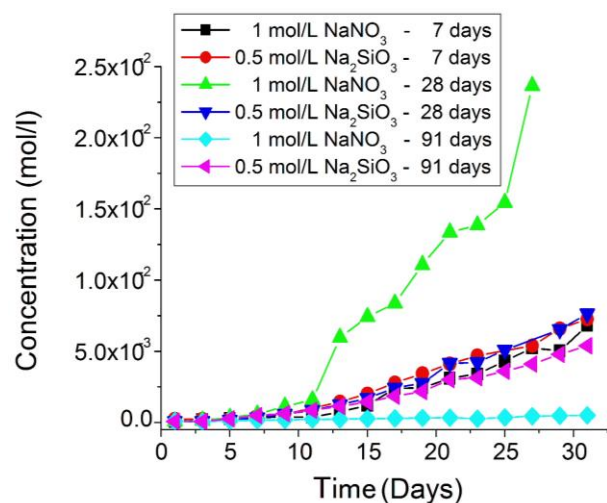


Fig. 4 Diffusion profiles of Na<sup>+</sup> ions from NaNO<sub>3</sub> and Na<sub>2</sub>SiO<sub>3</sub> solution (curing time: 7, 28 and 91 days)

### 3.1.2 Diffusion starting time (DST)

The result of DST of various lithium and sodium compounds is given by Fig. 5. DST was directly proportional to curing time, especially for  $\text{LiNO}_3$  solution. However it was delayed on DST of  $\text{LiNO}_3$  solution. DST of  $\text{LiNO}_3$  solution increased from 9 days in 7 days cured samples to 13 days in 28 days cured samples and to 17 days in 91 days cured samples. In case of  $\text{Na}_2\text{SiO}_3$  solution, DST averaged in 5 days. It is also important to note that the determination of DST in the latter is fairly a difficult task, because  $\text{Na}^+$  ions are immediately released from the pore solution of cement pastes. Thus it is difficult to distinguish whether the  $\text{Na}^+$  ions are from the solution or from the pore solution of cement pastes.

### 3.1.3 Diffusion coefficients ( $D_e$ )

Fig. 6 shows the effective diffusion coefficients ( $D_e$ ) of lithium ( $\text{Li}^+$ ) ions from  $\text{LiNO}_3$  and  $\text{Li}_2\text{SiO}_3$  solutions and also the effective diffusion coefficients ( $D_e$ ) of sodium ( $\text{Na}^+$ ) ions from  $\text{NaNO}_3$  and  $\text{Na}_2\text{SiO}_3$  solution in 7, 28 and 91 days cured OPC-0.4 specimens, calculated by Fick's 1st Law. In general, the diffusion coefficients of  $\text{Na}^+$  ions were 10 times more than  $\text{Li}^+$  ions.  $D_e$  of  $\text{Li}_2\text{SiO}_3$  and  $\text{Na}_2\text{SiO}_3$  compounds shows the similar diffusion behavior. The coefficients of both compounds were decreasing over time. However,  $D_e$  of both  $\text{LiNO}_3$  and  $\text{NaNO}_3$  compounds were low in the beginning, due to its absorption into the reaction products and then the coefficients increased over time but decreased again after 28. It might be due to the fact that the formation of calcium silicate hydrates have already stabled.

### 3.1.4 Differential scanning calorimetry analysis (DSC)

Differential Scanning Calorimetry analysis (DSC) was carried out upon diffusion test completion, with a Thermo-plus DSC 8270 equipment. The temperature range was from  $20^\circ\text{C}$  to  $1.000^\circ\text{C}$ , with a heating rate of  $10^\circ\text{C}/\text{min}$ . The specimens were previously finely ground ( $<150\mu\text{m}$ ) and vacuum dried for a minimum 24 hour period and each sample weight was set at 42 mg. DSC curves of OPC-0.4 specimens subjected to diffusion tests with various lithium and sodium compound solutions at 7 days are shown in Fig. 7. The formation of ettringite (Ett) was confirmed by a peak between  $75^\circ$  and  $150^\circ\text{C}$  in all specimens. Peaks which similar to Friedel's salt (FSt) were observed in  $\text{LiNO}_3$  and  $\text{NaNO}_3$  specimens. By exchanging chloride ( $\text{Cl}^-$ ) with nitrate ( $\text{NO}_3^-$ ) ions, the new compound formula turns into  $3\text{CaO}\cdot\text{Al}_2\text{O}_3\cdot\text{Ca}(\text{NO}_3)_2\cdot 10\text{H}_2\text{O}$ . In terms of residual CH, the following increasing order was observed:  $\text{NaNO}_3 < \text{LiNO}_3 < \text{Na}_2\text{SiO}_3 < \text{Li}_2\text{SiO}_3$ . Between  $670^\circ\text{C}$  and  $770^\circ\text{C}$ , Small calcium carbonate peaks ( $\text{CaCO}_3$ ) were observed in all specimens. These peaks are result of carbonation of CH due to possible exposure and contamination with  $\text{CO}_2$  during the analysis.

### 3.1.5 X-ray diffraction analysis (XRD)

Powder X-ray diffraction analysis was conducted to investigate the formation of hydration products. The

diffraction patterns were recorded by a XD-D1 diffractometer (Shimadzu).  $\text{CuK}\alpha$  radiation was used at a voltage of 40 kV and a current of 20 mA. The measurements were carried out in a  $2\theta$  range of  $5^\circ$  to  $40^\circ$ , with a scan speed of 2 degrees per second. Result of XRD patterns of OPC-0.4 specimens subjected to diffusion tests of various lithium and sodium compounds at 7 days are shown by Fig. 8. Ettringite peaks (Ett) were observed at  $8.8^\circ$ ,  $15.6^\circ$  and  $23^\circ$  in all specimens. At  $11.2^\circ$ , peaks which resemble Friedel's salt (FSt) were observed in  $\text{LiNO}_3$  and  $\text{NaNO}_3$  specimen. Residual calcium hydroxide (CH) was confirmed by sharp peaks at  $18^\circ$  and  $34^\circ$  with the following increasing order was observed:  $\text{NaNO}_3 < \text{LiNO}_3 < \text{Na}_2\text{SiO}_3 < \text{Li}_2\text{SiO}_3$ . These findings are confirming the results obtained from the DSC analysis.

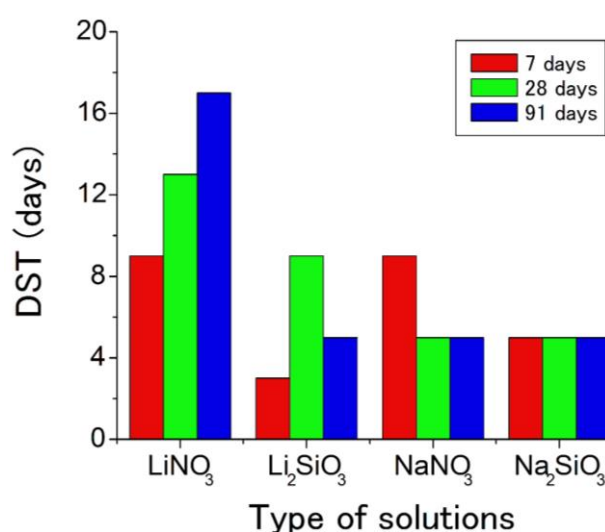


Fig. 5 Diffusion starting time (DST) of various lithium and sodium compounds

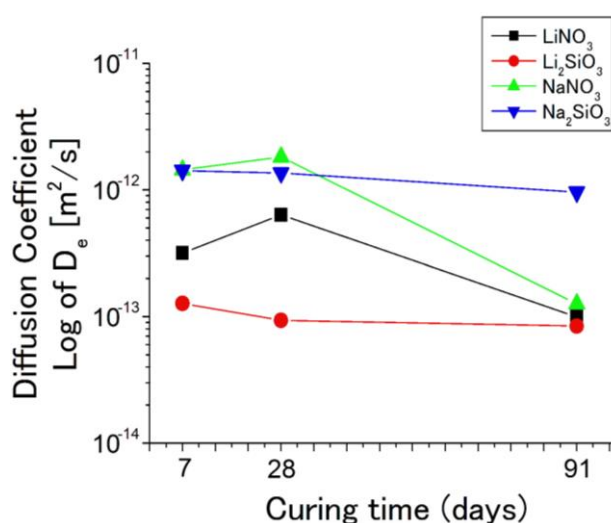


Fig. 6 Diffusion coefficients of  $\text{Li}^+$  and  $\text{Na}^+$  from various lithium and sodium compounds (curing time: 7, 28 and 91 days)



### 3.2 Accelerated Mortar Bar Test According to ASTM C1260

#### 3.2.1 Expansion ratio of mortar bars immersed in lithium and sodium solutions

In this experiment, accelerated mortar bar tests in accordance to ASTM C1260 method were conducted for specimens ( $25 \times 25 \times 285\text{mm}$ ) immersed in  $\text{Li}_2\text{SiO}_3$ ,  $\text{Na}_2\text{SiO}_3$  and  $\text{NaNO}_3$  solution. As shown in Fig. 9, regardless of concentrations, the specimens immersed in  $\text{Li}_2\text{SiO}_3$  solution did not expand at all, which suggests no ASR occurrence. Furthermore, a very interest phenomenon occurred in sodium solution. Specimens immersed in 0.5 mol/L  $\text{Na}_2\text{SiO}_3$  solution exceeded 0.2% at 14 days and surpassed 0.4% after 28 days period. As for specimens immersed in 1 mol/L  $\text{NaNO}_3$ , even though there was no expansion until 14 days, but the specimen expands and surpassed 0.3% after 28 days period. On the contrary, for specimens immersed in 2.5 mol/L  $\text{Na}_2\text{SiO}_3$  solution, only an early small expansion was observed and over curing time this expansion vanished. In addition, unlike the 0.5 mol/L  $\text{Na}_2\text{SiO}_3$  solution, which at  $80^\circ\text{C}$  is in the liquid state, 2.5 mol/L  $\text{Na}_2\text{SiO}_3$  solution revealed a very high viscosity and remained in paste-like state up to 14 days.

It is likely that, at the early stages, the ability of this high-concentrated water-glass solution to penetrate the specimens is compromised, while at the presence of highly reactive flint aggregates, the hydrolysis reaction of sodium compound and water to produce  $\text{NaOH}$  is raising the alkalinity in pore solution, which also increases the  $\text{OH}^-$  in the solution, thus triggers the occurrence of ASR. However, continuing supplied by high concentration of  $\text{Na}_2\text{SiO}_3$  from the outside make the reaction between  $\text{Na}_2\text{SiO}_3$  and  $\text{Ca}(\text{OH})_2$  take place and surpasses the pace of alkali-silica reaction. The overwhelming amount of C-S-H gel produced engulfs and surrounds the ASR-gel previous produced, and the ASR-induced expansion is suppressed. This phenomenon is different to that observed in the presence of lithium compounds, because the highly reactive lithium prevents ASR occurrence in the first place.

#### 3.2.2 Differential scanning calorimetry analysis (DSC)

Figs. 10 and 11 show the DSC curves of mortar bars immersed in 0.5 mol/L and 2.5 mol/L  $\text{Li}_2\text{SiO}_3$  and  $\text{Na}_2\text{SiO}_3$  solutions respectively. Around  $450^\circ\text{C}$ , a CH peak was observed. At about  $800^\circ\text{C}$  decarbonation of calcite, which is present in the limestone aggregates, was observed. However, ettringite peaks ( $\text{E}_{\text{tt}}$ ) were not detected due to thermal curing in the solutions at  $80^\circ\text{C}$  for 28 days. In the case of  $\text{Li}_2\text{SiO}_3$  solution, the residual amount of CH tended to more and directly proportional to solution concentration. This may be evidence that lithium ions ( $\text{Li}^+$ ) exchanged calcium ions ( $\text{Ca}^{2+}$ ) from the C-S-H gels and the released calcium ions precipitated into calcium hydroxide (CH), thus leading to more residual CH in the cement pastes. The DSC analysis of mortar bars immersed in 2.5 mol/L  $\text{Na}_2\text{SiO}_3$  solution was divided in two parts. The residual CH peak area in the “outer” curve was similar to that observed in the specimens immersed in 0.5 mol/L  $\text{Na}_2\text{SiO}_3$  solution.

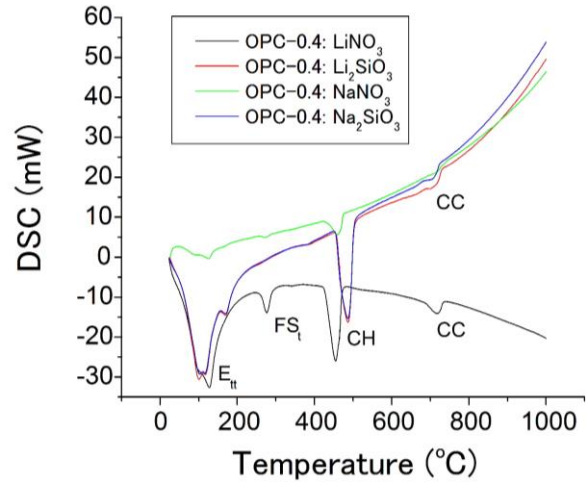


Fig. 7 DSC curves subjected to diffusion test of various lithium and sodium compounds (curing time: 7 days)

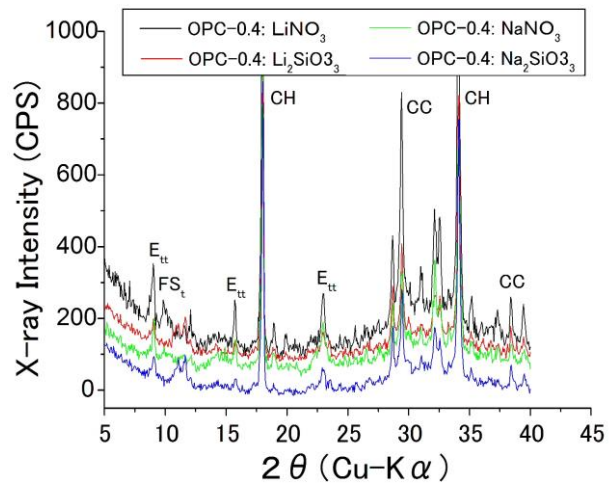


Fig. 8 XRD patterns subjected to diffusion test of various lithium and sodium compounds (curing time: 7 days)

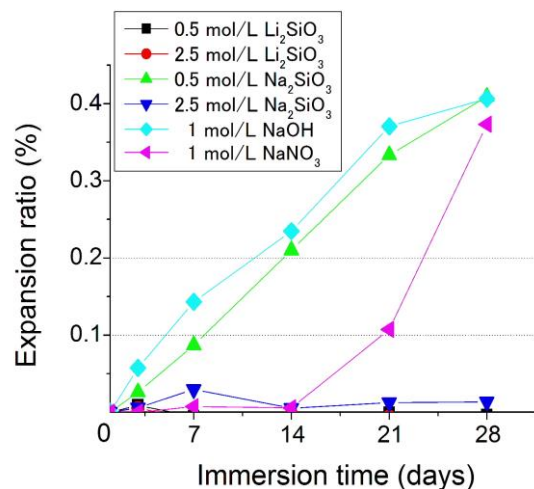


Fig. 9 Expansion ratio of accelerated mortar bars immersed in various lithium and sodium compounds according to ASTM C1260

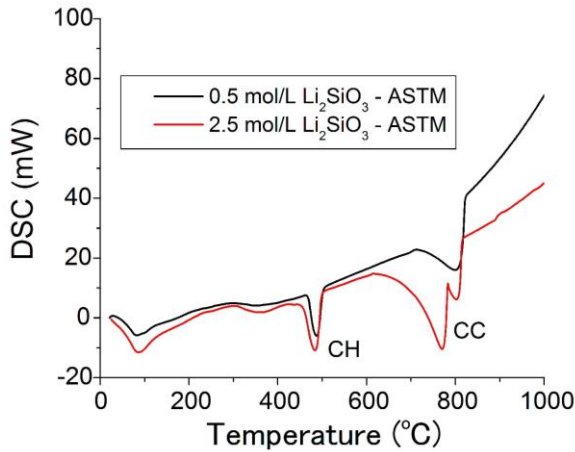


Fig. 10 DSC curves subjected to mortar bars immersed in 0.5 mol/L and 2.5 mol/L  $\text{Li}_2\text{SiO}_3$  solutions (immersion time: 28 days)

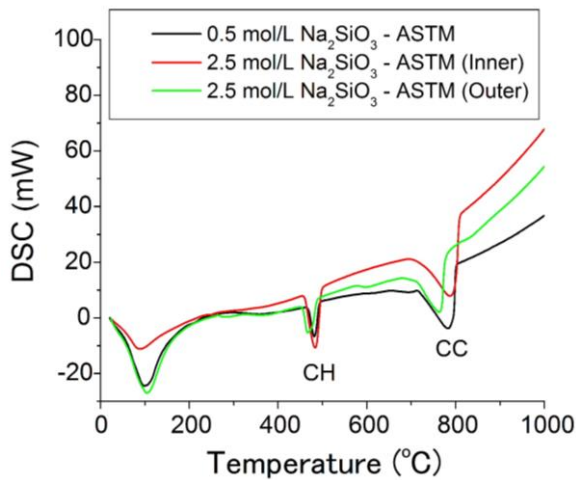


Fig. 11 DSC curves subjected to mortar bars immersed in 0.5 mol/L and 2.5 mol/L  $\text{Na}_2\text{SiO}_3$  solutions (immersion time: 28 days)

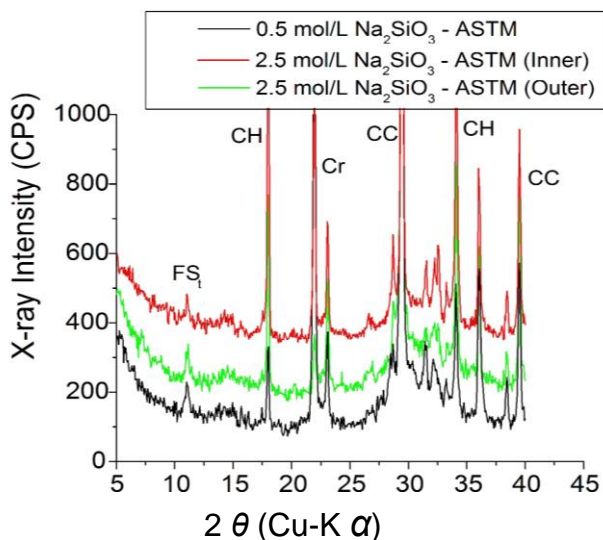


Fig. 12 XRD patterns subjected to mortar bars immersed in 0.5 mol/L and 2.5 mol/L  $\text{Na}_2\text{SiO}_3$  solutions (immersion time: 28 days)

Both curves were less than the one in the “inner” curve. This could be indicative that ASR occurred to a greater extent in the former than in the latter.

### 3.2.3 X-ray diffraction analysis (XRD)

XRD patterns of mortar bars immersed in 0.5 mol/L and 2.5 mol/L  $\text{Na}_2\text{SiO}_3$  solutions are shown in Fig. 12. Overall, XRD patterns are showing the same result as DSC curves. Residual calcium hydroxide (CH) was confirmed by sharp peaks at  $18^\circ$  and  $34^\circ$ . No ettringite peaks (Ett) were detected. In addition, sharp peaks believed to be  $\alpha$ -quartz were observed at  $22^\circ$ . This believe as the reactive aggregate used in the mortar bar tests, and may have ended mixed up with the portions of cement pastes selected for the XRD analysis.

### 3.2.4 Electron probe micro-analysis of mortar bars immersed in $\text{Na}_2\text{SiO}_3$ solution

The mapping imagery of sodium (Na) and silica (Si) in mortar bars immersed in 0.5 mol/L and 2.5 mol/L  $\text{Na}_2\text{SiO}_3$  solutions obtained by EPMA analysis is shown in Fig. 13. Electron probe microscope analysis (EPMA) of thin sections was conducted to obtain more understanding in the occurrence of ASR in specimens immersed in 0.5 mol/L and 2.5 mol/L  $\text{Na}_2\text{SiO}_3$  solution. EPMA results confirmed that ASR indeed occurred in both specimens, but was later suppressed in the outer-section of mortar bars immersed in 2.5 mol/L  $\text{Na}_2\text{SiO}_3$  solutions. In the case of 0.5 mol/L  $\text{Na}_2\text{SiO}_3$  solution, although ASR-gel was observed covering the entire section, the amount of Na is quite low and is similar to the one observed in the inner-section of mortar bars immersed in 2.5 mol/L  $\text{Na}_2\text{SiO}_3$  solution. However, the reflections of Na in the outer-section were far more, which combined with the low silica (Si) content in this part, suggests that ASR occurred, although ASR-gel could not be detected by uranyl acetate fluorescence method. High silica content in the inner-section of specimens immersed in 2.5 mol/L solution is indicative of un-reacted flint particles. These findings, confirmed the underlying ASR mitigation mechanism of  $\text{Na}_2\text{SiO}_3$  solution.

### 3.2.5 ASR gel formation in mortar bars immersed in lithium and sodium solutions

Uranyl acetate fluorescence method of coloring area was carried out to measure. The image of ASR gel observation in mortar bars immersed in lithium and sodium solutions by uranyl acetate fluorescence method is shown in Fig. 14. It shows no ASR gel could be found in  $\text{Li}_2\text{SiO}_3$  concentration, regardless of its concentrations. Suggesting again that no ASR occurs in  $\text{Li}_2\text{SiO}_3$  specimens. In the case of specimens immersed in 0.5 mol/L  $\text{Na}_2\text{SiO}_3$  and 1 mol/L  $\text{NaNO}_3$  solution, the whole cross-section is covered by dense spots of ASR gel. As for mortar bar immersed in 2.5 mol/L  $\text{Na}_2\text{SiO}_3$  solution, ASR gel was only observed in the inner-section of the mortar bars. It confirmed that ASR indeed occurred in this specimen, but it was later suppressed in the outer-section of mortar bars immersed in 2.5 mol/L  $\text{Na}_2\text{SiO}_3$  solutions. Due to huge amount of C-S-H gel produced that could sunk the ASR gel.

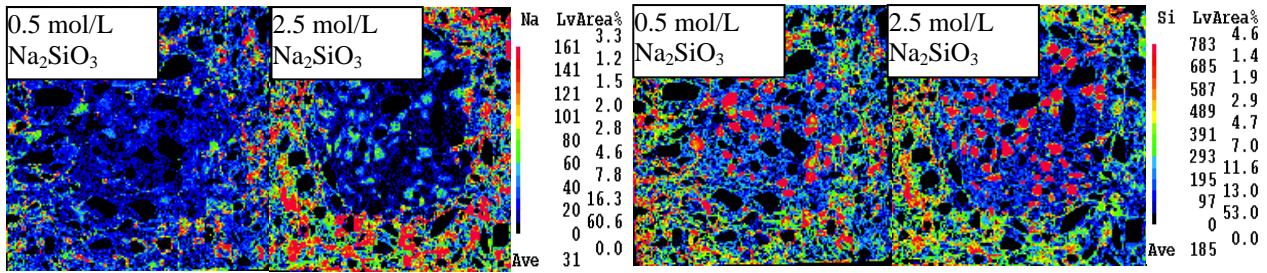


Fig. 13 Mapping imagery of sodium (Na) and silica (Si) in mortar bars immersed in 0.5 mol/L and 2.5 mol/L  $\text{Na}_2\text{SiO}_3$  solutions obtained by EPMA analysis (observed area: 25 mm x 25 mm)

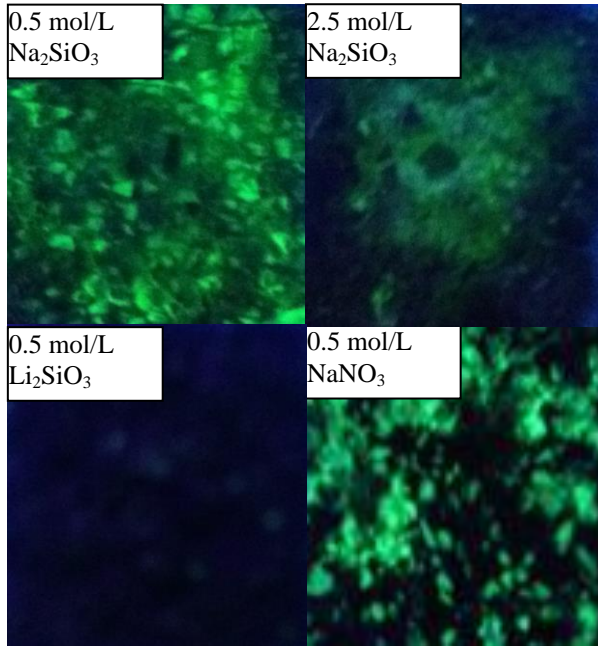


Fig. 14 Observations of ASR gel formation in mortar bars immersed in lithium and sodium solutions by uranyl acetate fluorescence method (observed area: 25 mm x 25 mm)

#### 4. CONCLUSIONS

- (1) The diffusion starting time (DST) of  $\text{Li}_2\text{SiO}_3$ ,  $\text{Na}_2\text{SiO}_3$  and  $\text{NaNO}_3$  was fast, around 3 until 9 days. As for  $\text{LiNO}_3$  solution, the DST was delayed compare to others.
- (2) The diffusion coefficients of  $\text{Na}^+$  ions were 10 times more than  $\text{Li}^+$  ions. This result could be indicative that lithium compounds reacts well and is better absorbed into the hydration products than sodium compounds, especially for  $\text{Li}_2\text{SiO}_3$  compound.
- (3) In terms of mortar bar expansion, regardless of  $\text{Li}_2\text{SiO}_3$  concentration, the specimens did not expand at all, which suggests no ASR occurrence.
- (4) After various of analysis conducted and the cost-effectiveness of these compounds.  $\text{Li}_2\text{SiO}_3$  can be proposed for mitigation of ASR-induced expansion in concrete while  $\text{Na}_2\text{SiO}_3$  can be proposed for mitigation of ASR-induced expansion in concrete only if it is in high concentration.

#### ACKNOWLEDGEMENT

The authors would like to express our deep gratitude to Dr. Eng. Osvaldo Andrade for his cooperation and contribution.

#### REFERENCES

- [1] NZ Transport Agency, "The influence of surface treatments on the service lives of concrete bridges." NZ Transport Agency, Wellington, 2010.
- [2] Dai, J. G., Y. Akira., Wittman F. H., Yokota H., and Zhang P., "Water repellent surface impregnation for extension of service life of reinforced concrete structures in marine environments: the role of cracks." *Cement and Concrete Composites*, Vol. 32, No.2, 2010, pp. 101–109.
- [3] Tremblay, C., Bérubé, M.A., Fournier, B., Thomas, M.D., and Folliard, K.J., "Experimental investigation of the mechanisms by which  $\text{LiNO}_3$  is effective against ASR." *Cement and Concrete Research*, Vol. 40, 2010, pp. 583-597.
- [4] Kawamura, M., and Fuwa, H., "Effect of lithium salts on ASR gel composition and expansion of mortars." *Cement and Concrete Research*, Vol. 33, 2003, pp. 913-919.
- [5] Diamond, S., and Ong, S., "The mechanisms of lithium effects on ASR." *Proceedings of the 9<sup>th</sup> International Conference on Alkali Aggregate Reaction*, Concrete Society of U.K., London, 1992, pp. 269-278.
- [6] Andrade, O., Prasetya, I., and Torii, K., "The diffusivity of lithium compounds through cement pastes and its effects on ASR mitigation." *Proceedings of ASEA-SEC-1*, Perth, 2012, pp. 463-468.
- [7] Yamato, H., Liu, Y., Omura, T., and Torii, K., "Mechanisms of ASR Deterioration Caused by Alkaline Salt Solution at High Concentration." *Cement Science and Concrete Technology*, Vol. 63, 2009, pp. 393-399. (In Japanese)